A deep inelastic neutron scattering study of sodium

1994 J. Phys.: Condens. Matter 6 2977

(http://iopscience.iop.org/0953-8984/6/16/003)

J. Phys.: Condens. Matter 6 (1994) 2977–2984. Printed in the UK

A deep inelastic neutron scattering study of sodium

S Fulton†, R A Cowley† and A C Evans‡
† Clarendon Laboratory, Physics Department, Oxford University, UK
‡ Rutherford Appleton Laboratory, Chilton, Didcot, Oxon OX11 0QX, UK

Received 4 February 1994

Abstract. Using the high-energy neutrons available at the ISIS facility, a deep inelastic neutron scattering study of polycrystalline sodium has been made. In this experiment the scattering function, $S(Q, \omega)$, has been measured at four different temperatures (30 K, 100 K, 200 K, 300 K) in order to study the changes in the neutron Compton profiles. The data were analysed using the impulse approximation and the known density of states. Within the 4% accuracy of the experiment, the results are consistent with sodium behaving as a harmonic solid.

1. Introduction

Spallation sources produce an abundance of neutrons with energies in the 1–50 eV region of the spectrum, and these allow a direct determination of atomic momentum distributions by use of a technique known as deep inelastic neutron scattering (DINS). This technique requires high energy and momentum transfers in order that the impulse approximation (IA) can be used to interpret the scattering data. The first studies using the IA were made on liquid ^{4}He [1–3] following the proposal made by Hohenberg and Platzman [4] that it enabled the proportion of atoms in the zero-momentum state of the superfluid to be determined. The development of spallation sources with high-energy neutron intensities, two orders of magnitude larger than those from reactor sources in the 1–50 eV region, has now made it possible to make similar measurements on light atoms in crystals [5, 6].

At the Rutherford Appleton Laboratory's ISIS facility, the inverse geometry spectrometer EVS has been developed for doing work in the high-energy regime required to analyse impulsive recoil scattering. The purpose of our experiment on sodium was to study the temperature dependence of the atomic momentum distribution and to compare the results with calculations based on the harmonic approximation and the known density of phonon states [7]. When this comparison was made in solid helium [8] the widths observed were 15% larger than those calculated and the difference was attributed to anharmonic effects in the phonon momentum distribution, and thus the calculation based on the harmonic theory were inadequate. A similar comparison has been made in the case of beryllium [5] and lithium [9] on the HET instrument at ISIS, and in these experiments the widths were 6% and 12% larger than theory. However, an experiment performed on lithium using the EVS spectrometer gave measurements less than 2% larger than the theory [6]. One explanation for these larger widths is that the harmonic approximation for the atomic momentum distribution may be affected by anharmonicity. In sodium [10] anharmonic effects are large at high temperatures, and a comparison between the measured width and the calculated width will provide further information above the effects of anharmonicity and the validity of interpreting the IA in terms of the harmonic model.

0953-8984/94/162977+08$19.50

2. Theory

The IA assumes that when at atom in a system collides with a high-energy neutron, the scattering atom recoils freely and the effects of interatomic collisions can be neglected [11]. The dynamic structure factor $S(Q, \omega)$ may be written

$$S(Q, \omega) = \int n(p)\delta\left[\hbar\omega - \frac{\hbar^2 Q^2}{2M} + \frac{\hbar^2 p \cdot Q}{M}\right]\mathrm{d}p. \tag{1}$$

This represents the incoherent scattering from a system of free particles with a momentum distribution $n(p)$. In this equation, $\hbar p$ is the initial momentum of an atom in the target system, $\hbar Q$ is the momentum transferred from the neutron to the sample, $\hbar\omega$ is the energy transfer, and M is the atomic mass of the scattering system.

For an ideal solid with harmonic interatomic interactions the IA is valid asymptotically at high wavevector transfers [12]. The theory then predicts [13] that for a monatomic system the high-energy wavevector scattering is given by

$$S_{\mathrm{IA}}(Q, \omega) = \left(1/2\pi\sigma_s^2\right)^{1/2} \exp\left(-\left(\hbar\omega - \hbar^2 Q^2/2M\right)^2/2\sigma_s^2\right) \tag{2}$$

a Gaussian centred at a recoil energy of $\hbar^2 Q^2/2M$ for a wavevector transfer Q, with width $\sigma_S = \hbar^2 Q \cdot p/M$, where $\hbar p/M$ is the root mean square initial velocity of the atom. The Q^2 dependence of the recoil energy and the Q dependence of the width can be used to check the validity of the IA. The slope of the width, σ_S, versus Q gives the mean momentum of the atoms, which can be directly compared with the theory.

It is useful to introduce an analysis technique for DINS known as y-scaling [14] where

$$y = (M/Q)\left(\omega - \hbar Q^2/2M\right). \tag{3}$$

In the y-scaling transformation every point in (Q, ω) space corresponds to a unique point in the atomic momentum space $\hbar p$. For an isotropic system the following relations hold:

$$S(Q\omega) = (M/Q)J(y) \tag{4}$$

$$J(y) = \int n(p_x, p_y, y)\mathrm{d}p_x\,\mathrm{d}p_y \tag{5}$$

where the z-axis has been taken along the direction of the wavevector transfer, Q. $J(y)$ is known as the neutron Compton profile and is analogous to the Compton profile for x-ray scattering [15]. Consequently $J(y)$ is the probability that an atom has the momentum component y along Q.

For an isotropic harmonic system the atomic momentum distribution is identical to that for an ideal gas, except that the temperature T is replaced by T^*—an effective temperature [16]. Thus $n(p)$ is given by

$$n(p) = \left(1/2\pi M k_{\mathrm{b}} T^*\right)^{3/2} \exp\left(-p^2/2M k_{\mathrm{b}} T^*\right) \tag{6}$$

$$k_{\mathrm{b}} T^* = \frac{1}{2}\int \hbar\omega Z(\omega) \coth\left(\frac{\hbar\omega}{2k_{\mathrm{b}}T}\right)\mathrm{d}\omega. \tag{7}$$

In this equation, $Z(\omega)$ represents the density of states of the lattice vibrations. Substituting equations (6) and (7) into equation (5) we have that the neutron Compton profile for an isotropic harmonic system has the following Gaussian form:

$$J(y) = \left(1/2\sigma_y\right)^{1/2} \exp\left(-y^2/2\sigma_y\right) \tag{8}$$

with the width σ_y given by

$$\sigma_y = \left(Mk_bT^*\right)^{1/2}. \tag{9}$$

Note that the width of the $J(y)$, σ_y, is equal to $\hbar y$—the initial z-component of the momentum of an atom in the target system. For an isotropic harmonic solid the width of the neutron Compton profile is Q independent and this means that the widths from different detectors can be averaged together.

If the density of states, $Z(\omega)$, for a system is known it is a simple matter to compare the widths extracted from the neutron Compton profiles with equations (7) and (9)—assuming the IA is valid.

3. The experiment

The sodium used was polycrystalline and was placed between two flat plates with vanadium windows such that the sample thickness was 5 mm. At this thickness the sodium gave about 4% scattering—low enough that multiple-scattering effects were not significant [5]. The sample can was placed in a cryostat in order that the neutron Compton profile could be measured at various temperatures (30 K, 100 K, 200 K, 300 K) to observe the systematic changes in the widths with increasing temperature.

The data to measure the atomic momentum distribution of sodium were collected as time-of-flight spectra on the EVS spectrometer at the Rutherford Appleton Laboratory. This has a large flux of high-energy neutrons, as required for DINS. EVS has four banks of ^{3}He detectors, two in the forward-scattering position (±36–±54°) and two in the back scattering (±140–±152°). The forward-scattering banks contain ten detectors each and the back-scattering banks fifteen. The source-to-sample distance on EVS is 11 m, the distance from the sample to the forward-scattering detectors is 0.8 m, and for the back scattering detectors it is 1 m. The experiment was set up using two different types of analyser foil—gold and uranium, positioned such that each covered a forward- and back-scattering bank of detectors. The analyser foils use the nuclear resonance absorption (Au—4.922 eV, U—6.671 eV) to define the final energy of the scattered neutrons, and a filter difference technique is used to collect the data. The foils give different energy resolutions because they have different resonance widths (FWHM: ΔE_{Au} = 0.141 eV, ΔE_U = 0.061 eV). The uranium foils have better resolution, but lower transmission than the gold foils and thus result in worse statistics for equal counting times.

The energy component of the resolution function on EVS is Lorentzian in shape and is the dominant instrumental effect. It is dependent on the widths of the resonance of the foil, and in y-space also depends on the mass of the target system. In y-space when the mass of

the target system is much larger than the mass of a neutron of the HWHM of the Lorentzian energy contribution is given by [17]

$$\sigma_E = \left\{ M\left[1 + L_1/L_0\right]/2\hbar k_1 \sin(\Theta/2) \right\} \Delta E/2. \tag{10}$$

where L_1 is the sample-to-detector distance and L_0 is the source-to-sample distance, k_1 is the scattered neutron momentum, Θ is the scattering angle and ΔE is the resonance width of the analyser foil. Table 1 shows the energy resolution width for a detector from each of the four different banks of our experimental configuration. It is seen that the resolution from the back-scattering detectors is better than that from the forward-scattering banks, and that the uranium foils have better resolution than the gold.

Table 1. Energy resolution widths on EVS.

Scattering angle, Θ (°)	Gold foil, $\sigma_E/\hbar$ (Å^{-1})	Uranium foil, $\sigma_E/\hbar$ (Å^{-1})
44	23.0	9.5
145	9.3	4.0

The contribution of the recoil scattering is extracted from the neutron Compton profile by convolving the Lorentzian energy resolution function for each detector with a Gaussian giving a Voigt function. The angular resolution and the uncertainties due to the detector distances and time effects are included in the Gaussian function along with the width from the recoil scattering. For sodium these latter uncertainties give a small contribution to the widths compared to that from the resonance energy widths.

4. The data

The data were collected as time-of-flight spectra, with the analyser foil first in and then out. These two spectra were subtracted from each other before any other transformations were performed; the result is data at a fixed final energy as defined by the analyser foil. The procedure was then repeated with an empty can, and the result subtracted from the sample data. The time-of-flight data for each detector were transformed into (Q, ω) space using standard EVS routines described in [18]. The validity of the IA is tested by a graph of Q^2 versus the recoil energy, i.e. the peak position of $S(Q, \omega)$, as shown in figure 1 for each detector. The straight line is the prediction of the IA, $E_{\text{Recoil}} = \hbar^2 Q^2/2M$. The data points are from both the gold and uranium foil detectors at forward- and back-scattering angles. The back-scattering detectors do not lie exactly on the IA line—the uranium sitting slightly above and the gold slightly below. If these deviations were due to the failure of the IA both would be expected to lie on the same side of the line, for example any deviations from the IA due to final-state effects would result in data points that lay below the straight line [11]. It is thus concluded that there is no significant deviation from straight-line behaviour and

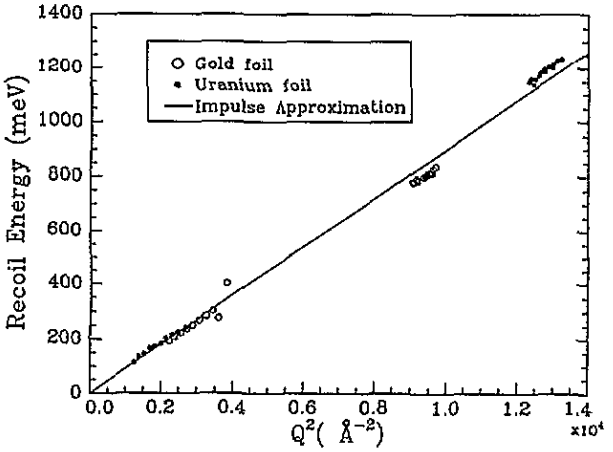

Figure 1. A graph of peak positions of $S(Q, \omega)$ versus Q^2. The straight line is a simulation using $E_{Recoil} = \hbar^2 q^2/2M$—the recoil energy from a harmonic solid. $T = 30$ K.

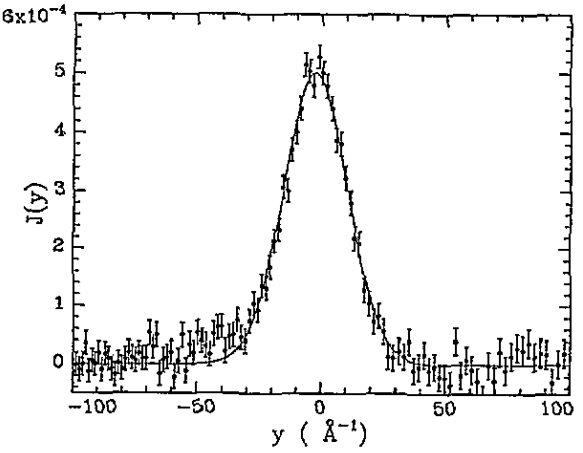

Figure 2. Transformed scattering data at 100 K from a forward-scattering detector with a gold foil analyser. The solid line represents a fit to a Voigt function.

that the discrepancies in the back-scattering detectors are due to errors arising in the data analysis, the can subtraction or instrument calibration.

The transformation to y-space was then performed [18]. The result of one of these transformations for a gold forward-scattering detector is shown in figure 2 along with a fit to a Voigt function—a Gaussian convolved with the Lorentzian energy resolution function as discussed in the previous section. Note that the recoil scattering is symmetric. The width of the recoil scattering was extracted from the Voigt function, and figure 3 shows these widths plotted against the detector angle for the uranium back-scattering bank. The widths of the neutron Compton profiles are independent of the detector angle within the experimental accuracy—the Q dependence having been removed by the y-scaling; this along with the Q^2 dependence of the peak positions (figure 1) shows that the data collected on EVS for

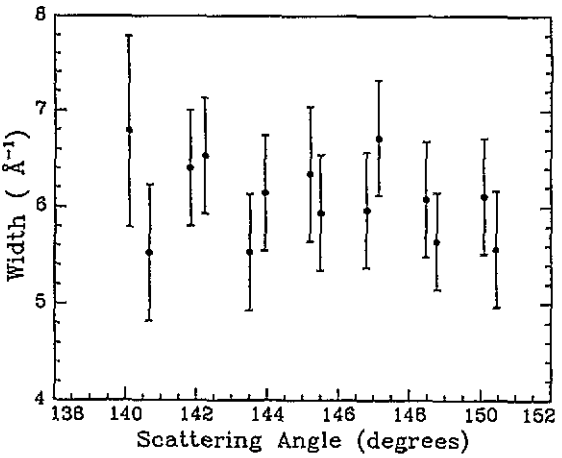

Figure 3. The width versus scattering angle for the uranium back-scattering detectors. Note that the width here is in units of $\sigma_y/\hbar = p$, and represents the initial momentum of the target system. T = 30 K.

sodium are consistent with the IA and hence that the analysis method is appropriate.

The widths extracted from the fits are known only to an accuracy of 6% for each detector in the back-scattering bank and 10% for the forward scattering. Since the Q-dependence has been removed by the y-scaling (figure 3), the widths from the detectors in each bank have been averaged. Figure 4 shows the temperature dependence of the widths along with a comparison of the theory for a harmonic solid (equation (9)) using the measured density of states [7] to calculate the effective temperature. Figure 4(a) shows that the widths from the gold high-angle detectors are systematically lower than the widths from the other banks; this is due to errors introduced when subtracting the empty-can run. Figure 4(b) shows the average widths from all four banks. Within the experimental spread of widths the data are well described by the theory and there is no evidence for any systematic deviations from harmonic solid behaviour. At 30 K, below the phase transition at 35 K from the body-centred cubic structure to the hexagonal close-packed structure [19], no evidence is seen for any appreciable change in the width.

The instrumental resolution of EVS in y-space deteriorates with target mass as given by equation (10), and so it will be difficult to obtain more accurate results for the recoil scattering for large masses, and hence to observe any deviations from the IA. In fact with the present resolution of EVS, accurate determinations of atomic momentum distributions are limited to atomic masses of less than 15 amu, with EVS being primarily useful for studying the momentum distribution of hydrogen and deuterium.

5. Conclusions

The EVS spectrometer has been used to show that the neutron recoil scattering from sodium below 300 K is consistent with the IA. Comparing the widths extracted from the neutron Compton profiles with the harmonic model for sodium, good agreement is seen within the accuracy of the data, ~4%, and thus from this experiment the recoil scattering from sodium is essentially the same as that from a collection of particles interacting with harmonic forces.

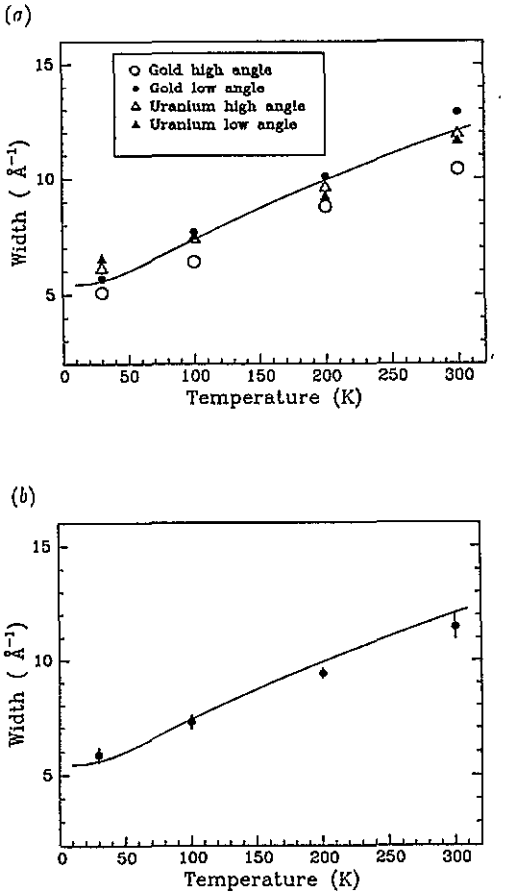

Figure 4. (*a*) The widths, $\sigma_y/\hbar$, extracted from the Voigt-function fits compared with a simulation of the theory for a harmonic solid, equation (9), using the measured density of states to calculate the effective temperature, T^*. (*b*) The average widths from the four banks.

Acknowledgments

We would like to thank Jerry Mayers for helpful discussions and advice during our time at the Rutherford Laboratory and also Mark Harris and Martin Zinkin for all their support and interest in this experiment. Financial support was provided by the Science and Engineering Research Council.

References

[1] Cowley R A and Woods A D B 1968 *Phys. Rev. Lett.* **21** 787
[2] Harling O K 1970 *Phys. Rev. Lett.* **24** 1046
[3] Mook H A, Scherm R and Wilkinson M K 1972 *Phys. Rev.* A **6** 2268
[4] Hohenberg P C and Platzman P M 1966 *Phys. Rev.* **152** 198
[5] McMorrow D F, Cowley R A, Nicklow R M, Mitchell P W, Taylor A D and Mostoller M 1990 *J. Phys. C: Solid State Phys.* **2** 1045
[6] Evans A C 1993 *Z. Naturf.* a **48** 425

[7] Dixon A E, Woods A D and Brockhouse B N 1963 *Proc. Phys. Soc.* **81** 973
[8] Hilleke R O, Chaddah P, Simmons R O, Price D L and Sinha S K *Phys. Rev. Lett.* 52 847
[9] Hewitt M 1989 *PhD Thesis* Edinburgh University
[10] Woods A D, Brockhouse B N, March R H and Stewart A T 1962 *Phys. Rev.* **128** 1112
[11] Mayers J 1989 *Europhys. Lett.* **10** 727
[12] Gunn J M F and Warner M 1984 *Z. Phys.* B 56 13
[13] Lovesey S W 1984 *Theory of Neutron Scattering from Condensed Matter* vol 1 (Oxford: Oxford University Press)
[14] Sears V G 1984 *Phys. Rev.* B **30** 44
[15] Williams B 1977 *Compton Scattering* (New York: McGraw-Hill)
[16] Nelkin M S and Parks D E 1960 *Phys. Rev.* **119** 1060
[17] Andreani C, Baciocco G, Holt R S and Mayers 1989 *J. Nucl. Instrum. Methods Phys. Res.* A **276** 297
[18] Mayers J and Evans A C 1991 *Rutherford Appleton Laboratory Report* RAL-91-048
[19] Martin D L 1960 *Proc. R. Soc.* A **254** 433